

The quantum spin Hall effect

Hartmut Buhmann^{a)}

Physikalisches Institut (EP3), Universität Würzburg, Am Hubland, 97074 Würzburg, Germany

(Received 9 August 2010; accepted 16 October 2010; published online 31 May 2011)

In a two-dimensional system the quantum spin Hall effect (QSHE) state is characterized by an insulating bulk and two counter-propagating helical edge states. These edge channels are protected by time reversal symmetry and spin currents propagate without dissipation. It was shown that HgTe-based quantum well structures are the most suitable candidates for its experimental realization. Here, the experimental requirements are discussed which lead to the observation of quantized edge channel transport which is one of the main signatures of the QSHE. Experiments will be presented which demonstrate the stability of the quantized conductance and its nonlocal character. Furthermore, evidence for the spin polarization of the QSHE edge channels is shown in an all-electrical measurement which demonstrates the potential of the QSHE for spin injection and detection applications in spintronics. © 2011 American Institute of Physics. [doi:10.1063/1.3577612]

I. INTRODUCTION

Spin polarization, manipulation, and detection are currently the most challenging tasks in semiconductor science. Spin injection in metals has already revolutionized data storage on hard disk drives.^{1,2} However, spin injection into semiconductors has turned out to be much more difficult. This is basically due to the facts that, on the one hand, the injection of a spin polarized electron from a ferromagnetic metal into a semiconductor is very inefficient due to the enormous mismatch of the density of states, and on the other hand, that only a few ferromagnetic semiconductor materials exist and Curie temperatures are mostly below 100 K. Thus, the search for spin polarizing effects in semiconducting materials guides many research activities.

So far, spin injection and spin valve behavior have been realized in magnetic semiconductors and ferromagnetic semiconductor tunnel devices.³ Another effect, the spin-orbit (SO) interaction, has recently been discussed as a candidate for spin polarization in semiconductors. The spin degeneracy can be lifted in crystals due to the lack of inversion symmetry. Two prominent effects are the bulk inversion asymmetry, or Dresselhaus-effect, and the structural inversion asymmetry. The latter is a dominant effect in quantum well (QW) structures and is known as the Rashba-effect.⁴ The symmetry of the QW potential is controllable to a large extent via external gate-voltages which makes this effect one possible candidate for spin-controlled transport in semiconductors. The most famous device concept in this context is the spin field effect transistor.⁵ However, for its realization, a controlled spin polarization, injection, and detection in semiconductor systems is required. Concepts like the spin Hall effect (SHE)⁶⁻⁹ and birefringent electron optics¹⁰ are explored with promising results.

Another effect, which demonstrates spin polarized charge transport, is the quantum Hall effect (QHE).¹¹ For odd filling factors (ν), and especially for $\nu = 1$, the current is

partially or fully spin polarized. The only drawback is that in order to create QHE states, the device has to be subjected to a high external magnetic field which disqualifies this effect from possible application purposes. An effect which provides well defined stable transport channels for spin polarized carriers similar to the QHE states would be more desirable.

In this presentation the so-called quantum spin Hall effect (QSHE) is introduced following the edge channel model which has been developed for the quantum Hall effect. It is shown that a band inversion is essential for its observation. Symmetry breaking at the edge of the sample leads to a gapless transition to a normal band structure ordering. Edge states are formed which allow for quantized spin dependent transport if the Fermi energy is located with the bulk excitation gap.¹² The QSHE has been proposed for narrow graphene stripes¹³ but at present has only been experimentally demonstrated for HgTe QW structures. In the following, the special band structure properties of HgTe are discussed and the experimental signatures of the QSHE are presented. The most important points are the precision of the conductance quantization and the spin polarization properties of the QSHE edge channels.

II. QUANTUM SPIN HALL EFFECT

The most successful illustration for the explanation of the experimental observations in the quantum Hall effect (QHE) regime is the concept of one dimensional edge channel transport. In the QHE regime the number of edge channels is given by the number of occupied Landau levels (LL). The quantized Hall conductance and the vanishing longitudinal resistance can be explained within the Landauer-Büttiker formalism.¹⁴ A schematic illustration for a QHE state of the filling factor $\nu = 1$ is given in Fig. 1(a) for two different directions of the magnetic field. In this illustration the QHE can be viewed as a first example of a topological insulator, since transport takes place at the edge of the sample while the bulk is insulating. In the case of the QHE, the Fermi energy is located in the gap between two Landau levels. The

^{a)}Author to whom correspondence should be addressed. Electronic mail: hartmut.buhmann@physik.uni-wuerzburg.de.

stability of the quantization effect is given by the fact that the left and right moving channels are located at opposite edges of the sample. Potential fluctuation at the edge of the sample will deflect the edge channels into the bulk region but backscattering is suppressed as long as the wave functions of the edge states do not overlap.

Using this simplified picture of the edge channel transport, the QSHE state can now be constructed from two copies of the QHE state, one for each spin component, as shown in Fig. 1(a). A combination of both states in a single sample will result in two counterpropagating edge modes with opposite spin [Fig. 1(b)]. This new state exists even without the magnetic field.¹² It should be noted that even though counterpropagating channels are now present at each edge, backscattering is not possible because these states form so-called Kramer’s doublets, $\Psi_{k,s^+}, \Psi_{-k,s^-}$, which are protected by time reversal symmetry. In order to introduce backscattering, either time reversal symmetry has to be broken, which can be done by a magnetic field, or the edge channels have to propagate through areas of finite electron or hole density, where scattering becomes possible.

The question which now arises is: In what kind of materials does the quantum spin Hall effect exist? The first candidate which was discussed in the literature was graphene.¹³ For certain narrow stripes of graphene, the existence of helical edge states has been predicted. However, due to the very small SO energy, the resulting insulating gap is far too small for QSHE edge channel transport to be observable with the current experimental techniques. However, in 2005, Bernevig *et al.*¹⁵ presented calculations which showed that the QSHE should be observable in HgTe QWs with an inverted sub-band structure ordering.

III. HGTE QUANTUM WELLS

Bulk HgTe is a semimetal with a degenerate heavy hole (HH) valence and a light hole (LH) conduction band state at

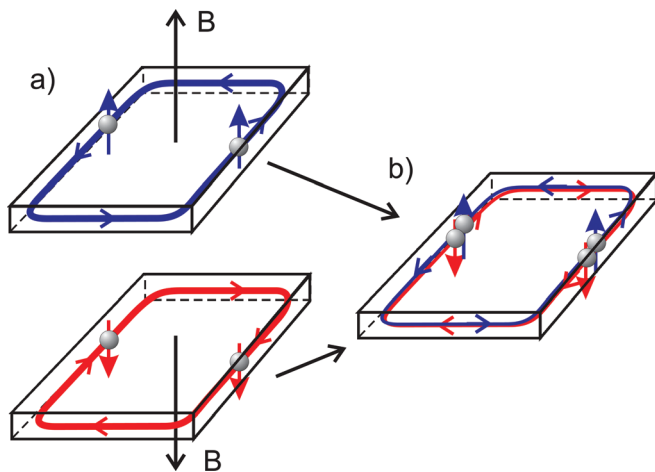


FIG. 1. (Color online) (a) Two copies of a $\nu = 1$ chiral QHE edge state for an inverted magnetic field. The long arrow indicates the direction of the magnetic field and short arrows indicate the spin polarization directions. (b) A combination of two $\nu = 1$ QHE states leads to a quantum spin Hall state without a magnetic field.

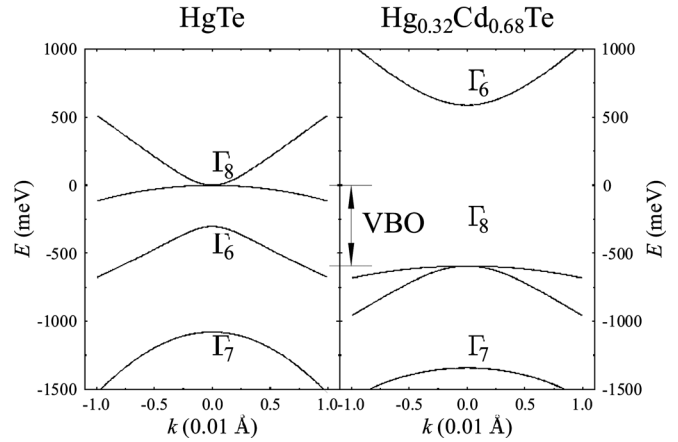


FIG. 2. Energy dispersion for the conduction and valence band of HgTe and HgCdTe near the Γ point. The valence band offset is indicated by arrows. (VBO \approx 570 meV).

the Brillouin zone center, the Γ -point (cf., Figure 2). Due to the strong SO coupling the p-orbital-like Γ_8 band is energetically lifted above the s-orbital-like Γ_6 band. The related energy difference is about 300 meV. Thus, HgTe might as well be viewed as a semiconductor with a negative bandgap ($E_g := E_{\Gamma_6} - E_{\Gamma_8} = -300$ meV).

If a thin layer of HgTe is embedded between $Hg_{1-x}Cd_xTe$ (with $x > 10\%$) the degeneracy between the LH and HH state is lifted and a gapped semiconductor is formed due to the quantum confinement. $Hg_{0.32}Cd_{0.68}Te$ is a normal gap semiconductor as shown in Fig. 2 (right panel). A HgTe/HgCdTe-quantum well (QW) forms a so-called type-III structure: The Γ_6 -like conduction band-edge is below the Γ_8 -like valence band-edge within the QW (Fig. 3). For wide wells the highest confined Γ_8 -like level, labeled HH1, is still above the lowest Γ_6 -like, labeled E1, and forms the lowest conduction band level. Such a situation is schematically shown in Fig. 3, which depicts a type-III QW with an inverted sub-band structure ordering. For a larger confinement the sub-band structure ordering becomes again normal i.e., $E_{E1} > E_{HH1}$. However, the observation of the quantum spin Hall effect requires an inverted sub-band structure ordering which is the case for QW widths, d , larger than 6.3 nm.¹⁶

At the edge of the sample the crystal symmetry is broken and the SO coupling strength is reduced. The Γ_6 -like

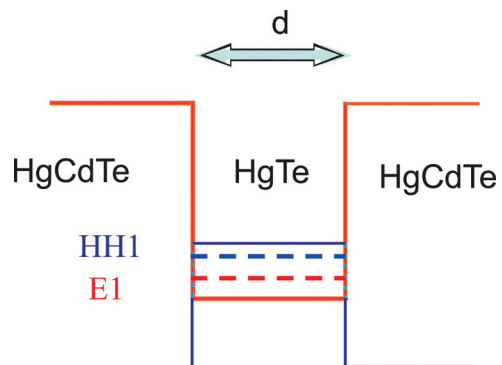


FIG. 3. (Color online) Type-III HgTe QW structure with inverted sub-band structure ordering: HH1 conduction and E1 valence band.

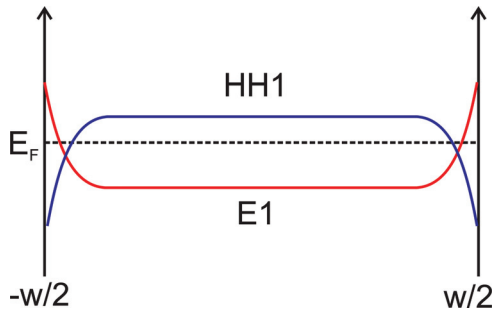


FIG. 4. (Color online) Schematic local energy dependence of the HH1- and E1-like band, forming one-dimensional counterpropagating edge channels.

and Γ_8 -like bands will return to their normal energetic ordering, i.e., a point near the edge of the sample exists where these two bands intersect. Thus, the structure will be gapless at the edges. The situation is schematically shown in Fig. 4. Tight binding calculations shows that these two counterpropagating channels possess anti-parallel spin states. These states form Kramer's pairs and give rise to the quantum spin Hall effect (QSHE).¹⁵

IV. MEASUREMENT OF THE QSHE

The existence of the QSHE edge states can be demonstrated when the Fermi energy is located within the bulk energy gap. Electronic transport is expected to be carried by edge channels. Since there are two counterpropagating channels at each side for opposite spin states, a current will be distributed along two opposite edges. For a simple two terminal device the current will be confined to two one-dimensional edge channels which gives rise to a quantized conductance of $2e^2/h$. For a Hall-bar geometry the situation is shown schematically in Fig. 5. Each color symbolizes one spin state. Electrons that enter from the left will propagate either through the left or right moving channel depending upon their spin polarization. Since no backscattering is expected to occur within the QSHE regime the measured conductance should be quantized even for a multi-terminal device.

For the first set of experiments a 7 nm wide HgTe-QW structure was used with n-type doping. The carrier concen-

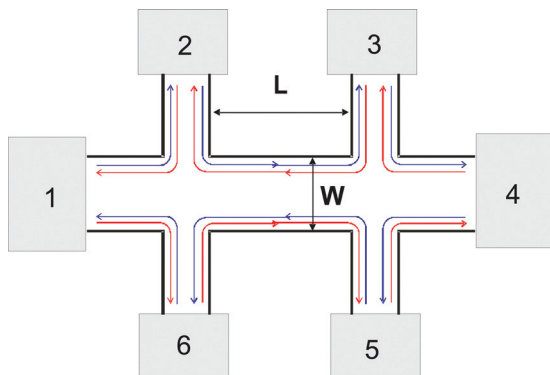


FIG. 5. (Color online) Multi-terminal device structure of width W and length L . The spin polarized edge channels are indicated in the QSH regime by arrows and the ohmic contact by numbers 1–6.

tration was $n_s \approx 3 \times 10^{11} \text{ cm}^{-2}$ and the carrier mobility was determined to be of the order of $\mu \approx 1.5 \times 10^5 \text{ cm}^2/(\text{Vs})$, which yields an elastic mean free path of $l_e \approx 1$ to $2 \mu\text{m}$. In order to assure that scattering potentials do not influence the carrier transport the samples were fabricated with dimensions of approximately the same order.

In general, edge channel transport is independent of the sample length, L , and width, W . Thus, various samples were fabricated for various aspect ratios. Note that all samples were equipped with a top gate electrode which allows for a continuous variation of the carrier density. The gate electrodes are only slightly larger than the devices. Thus, the contact regions remain n-type conducting which assures transport measurements with a metallic ohmic contact of constant resistance. Starting from a n-type conductance at zero gate-voltage the Fermi energy passes the bulk insulating regime for increasing negative gate-voltages and finally reaches a p-type conducting regime for voltages smaller than $V_g \leq -2$ to -4 V .

In Fig. 6 the results are shown for four-terminal measurements on three different devices. For all inverted QW devices the resistance $R_{14,23}$ reaches a value of $h/2e^2$ ($\approx 12.9 \text{ k}\Omega$) when the Fermi energy is located in the bulk insulating regime. Since the absolute value of the applied gate voltage, V_g , for the *n*-to-*p* transition differs slightly for individual samples, all measurements have been shifted by a constant offset, $V_{g,0}$. The maximum resistance now appears at a gate voltage of 0 V for all devices. For comparison, the maximum resistance $R_{14,23}$ of a QW structure with a normal band structure ordering ($d < 6 \text{ nm}$) reaches several megohms in this gate voltage regime (not shown here, see Ref. 16). The measured resistance value indeed suggests that a quantized conductance exists which does not depend upon the device dimensions. Note, that in the notation $R_{ij,kl}$ the indices *ij* denote the current and *kl* the voltage contacts.

In order to estimate the resistance value of a six-terminal device in four-probe geometry the Landauer-Büttiker formalism has been employed.¹⁴ Considering two counterpropagating edge channels and the fact that within the ohmic contacts

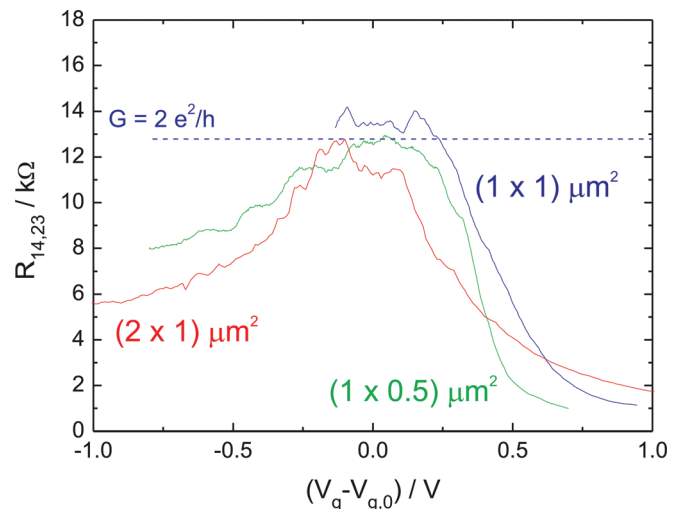


FIG. 6. (Color online) QSHE measurement for inverted QW structures. The device dimensions $L \times W$ are given in the figure.

backscattering takes place, the resistance can be calculated by using the following transmission matrix

$$T_{ij} = \begin{bmatrix} 0 & 1 & 0 & 0 & 0 & 1 \\ 1 & 0 & 1 & 0 & 0 & 0 \\ 0 & 1 & 0 & 1 & 0 & 0 \\ 0 & 0 & 1 & 0 & 1 & 0 \\ 0 & 0 & 0 & 1 & 0 & 1 \\ 1 & 0 & 0 & 0 & 1 & 0 \end{bmatrix}. \quad (1)$$

Solving the equation

$$I_i = e/h \sum_{j \neq i} T_{ij} (\mu_j - \mu_i), \quad (2)$$

yields $R_{14,23} = h/2e^2$, a value which has been observed for all measurements using this contact configuration.

Following the Landauer-Büttiker formalism it is possible to verify the ballistic edge channel transport concept of the QSH state by investigating different contact configurations. For example, from Eqs. (1) and (2) one infers that the resistance $R_{13,54}$ should be $h/3e^2 \approx 8.6 \text{ k}\Omega$. The agreement between the model and experiment is shown in Fig. 7. Additional contact configurations which confirm the nonlocality of the QSH effect can be found in Ref. 17.

V. STABILITY OF THE QSHE

It should be noted that despite the similarity between the quantum Hall effect and QSHE the conductance quantization in the latter case will strongly depend upon the quality of the samples. While in the QHE regime edge channel transport is unaffected by potential fluctuations, the quantized QSHE state may be destroyed. Generally, potential fluctuations raise or lower the Fermi energy. For narrow gap samples this may well introduce n- or p-conducting areas within the insulating regime. Since edge states of a topological insulator are not deflected from the sample edge by potential fluctuations, edge electrons will be injected into these metallic regions

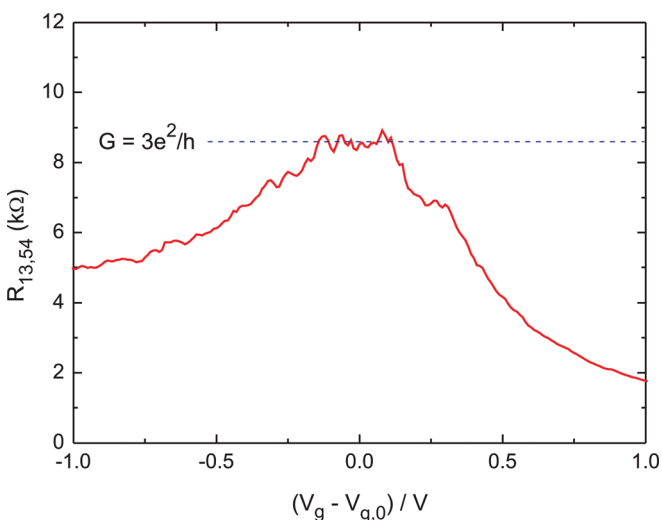


FIG. 7. (Color online) Quantized resistance for a two- ($R_{14,14}$) and four-terminal ($R_{14,23}$) measurement configuration in the QSH regime.

where backscattering becomes possible. This is in contrast to the quantum Hall state where the edge state is supposed to encircle the impurity on an equipotential line. The backscattering probability for the QSHE edge states depends upon the actual size and scattering strength of the impurity potential.¹⁷ The probability of finding such a metallic region at the sample edge increases with increasing device size and with decreasing sample quality. Thus, the device size and quality limits the observation of a quantized conductance in the QSH regime, especially in narrow gap samples.

The influence of potential fluctuations on the quantized conductance in the QSHE regime also depends on the actual energy gap and especially on the position of the Fermi energy with respect to the conduction and valence band-edge. Figure 8(a) gives a simple schematic illustration of the energy dispersion at the sample edge. If the Fermi energy is located at the midgap position the stability is largest. In the case of HgTe QWs the energy gap is of the order of 30 to 50 meV which is quite large and assures us that the QSH effect is observable for temperatures up to at least 4 K.¹⁸ However, the measurements show that even for high quality samples backscattering modulates the conductance value. In the current experiments the position of the Fermi level is changed by varying the gate voltage which is applied to a top electrode separated from the semiconductor by a 110 nm thick insulating SiO₂/Si₂N₃ multilayer. Trap states at the semiconductor insulator interface are charged or discharged by changing the gate voltage which influences the potential landscape within the quantum well. Consequently, continuously changing the potential landscape influences the backscattering probability of QSHE edge channel and thus, no constant well quantized conductance values are observable for these kinds of measurements. This explains the experimental observation displayed in Figs. 6 and 7.

Edge channel transport is also limited by the extension of the edge channel wave function into the bulk. If the sample width decreases below a certain limit the wave functions of opposite edges overlap and backscattering can take place.¹⁹ An estimation shows that this might happen for device sizes lower than 200–250 nm, which has been confirmed by measurements on narrow device structures.⁹

Additionally, the stability of the quantized QSHE state is influenced by an external magnetic field. The magnetic field destroys the time reversal symmetry and opens a gap in the edge channel energy dispersion. The strength of the gap

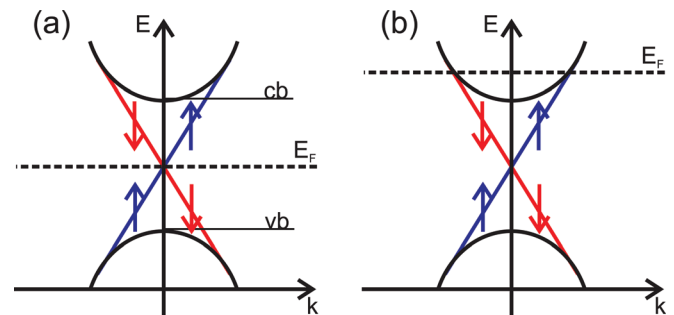


FIG. 8. (Color online) Schematic energy dispersion for QSH edge channels without (a) and with (b) external magnetic field.

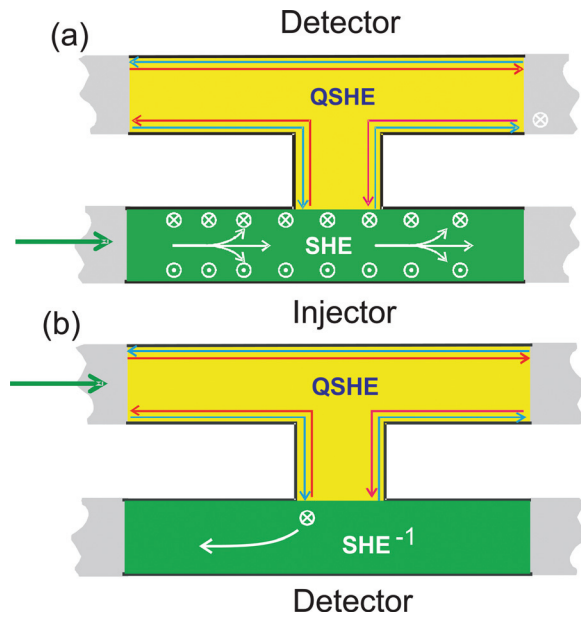


FIG. 9. (Color online) Schematic measurement configuration for the demonstration of the spin injection and detection properties of the QSH effect. Bright area: device region gate into the QSHE regime, dark area: metallic, either n- or p-type semiconductor.

depends upon the direction of the magnetic field relative to the plane of the QW.^{16,20} This influence is strongest if the magnetic field is applied perpendicular to the QW plane and decreases if the magnetic field vector is tilted into the plane of the QW.²⁰

VI. SPIN PROPERTIES

The remaining question is whether or not it is possible to use the QSHE for spin injection and detection purposes. In order to explore this possibility, the polarizing properties of the QSHE have been explored.

A QSHE system can be used to separate spin states in multi-terminal devices (cf., Figure 6). Thus, a multi-terminal device can easily be used to transport and to detect spin states and to inject spin states into a metallic (contact) regime. For the first demonstration, the spin polarizing properties of metallic n- or p-type HgTe QWs have been used. HgTe QWs exhibit one of the largest Rashba SO splitting energies for semiconductors. Rashba energies of up to 30 meV have been observed.²¹ In systems with a strong Rashba SO splitting the spin Hall effect (SHE) can be used to create distinct spin polarizations at the sample edges.^{7,8,22} The intrinsic SHE signal has recently been observed in HgTe QW structures in an all-electric measurements.⁹ However, it was observed that a spin related voltage signal was detectable only for the p-type conducting regime. For the n-type conducting regime the spin signal remained unresolved.⁹

The idea now is to combine the QSHE in the HgTe QW with the SHE by using split-gate technologies. Thus, the QSHE and the SHE regimes can be realized in close proximity. The schematic device structure and measurement configurations are shown in Fig. 9. This device can be used for spin detection as well as for spin injection experiments. In the first set of experiments, the SHE is used to create the

spin polarization by injecting a current into the metallic state. The spin accumulation at the edge of the sample is detected by the spin sensitive QSHE edge channels [Fig. 9(a)]. In a second set of experiments, a spin polarized current is injected from the QSHE regime into the metallic n- or p-type system. The inverse SHE (SHE^{-1}) creates a voltage signal due to the injected spin current [Fig. 9(b)].^{6,9} Measurements of all configurations confirm the spin dependent transport properties of the QSHE edge channels. Moreover, they reveal a very high spin sensitivity because a SHE signal became detectable even in the n-type conducting regime,²³ which has been unresolved in an all-electric SHE measurement configuration.⁹

VII. CONCLUSION

The quantum spin Hall effect (QSHE) is a new type of topological insulator state which exhibits distinct spin transport properties. The spin injection and highly sensitive spin detection properties show great potential for spintronics applications. The big advantages are that neither external magnetic fields nor magnetic materials or polarized light sources are required for the creation or detection of spin polarized carriers. Furthermore, spin states are transported without dissipation in ballistic one-dimensional edge channels.

Up to the present time this quantum spin Hall effect has only been experimentally demonstrated in HgTe quantum well systems, but the search for further materials with these extraordinary properties is in progress and we await new results.

ACKNOWLEDGMENTS

The experimental work on HgTe QW structures is done at the Physikalisches Institut, Lehrstuhl für Experimentelle Physik (Professor L.W. Molenkamp), Universität Würzburg, by the Quantum Transport Group (Professor H. Buhmann, C. Brüne, M. König, M. Leberecht, R. Rommel, A. Roth, and S. Wiedmann). For financial support, the Deutsche Forschungsgemeinschaft (Grant No. SPP 1285) is acknowledged.

¹M. N. Baibich, J. M. Broto, A. Fert, F. Nguyen Van Dau, and F. Petroff, *Phys. Rev. Lett.* **61**, 2472 (1988).

²G. Binasch, P. Grünberg, F. Saurenbach, and W. Zinn, *Phys. Rev. B* **39**, 4828 (1989).

³See, for example: D. D. Awschalom and M. E. Flatte, *Nat. Phys.* **3**, 153 (2007).

⁴Yu. A. Bychkov and E. I. Rashba, *Pis'ma Zh. Eksp. Teor. Fiz.* **39**, 66 (1984) [*JETP Lett.* **39**, 78 (1984)].

⁵S. Datta and B. Das, *Appl. Phys. Lett.* **56**, 665 (1990).

⁶J. E. Hirsch, *Phys. Rev. Lett.* **83**, 1834 (1999).

⁷Y. K. Kato, R. C. Myers, A. C. Gossard, and D. D. Awschalom, *Science* **306**, 1910 (2004).

⁸J. Wunderlich, B. Kaestner, J. Sinova, and T. Jungwirth, *Phys. Rev. Lett.* **94**, 047204 (2005).

⁹C. Brüne, A. Roth, E. G. Novik, M. König, H. Buhmann, E. M. Hankiewicz, W. Hanke, J. Sinova, and L. W. Molenkamp, *Nat. Phys.* **6**, 448 (2010).

¹⁰M. Khodas, A. Shekhter, and A. M. Finkel'stein, *Phys. Rev. Lett.* **92**, 086602 (2004).

¹¹K. v. Klitzing, G. Dorda, and M. Pepper, *Phys. Rev. Lett.* **45**, 494 (1980).

¹²C. L. Kane, E. J. Mele, *Phys. Rev. Lett.* **95**, 146802 (2005); C. Wu, B. A. Bernevig, and S. C. Zhang, *ibid.* **96**, 106401 (2006); C. Xu and J. Moore-Phys. Rev. B **73**, 045322 (2006).

¹³C. L. Kane and E. J. Mele, *Phys. Rev. Lett.* **95**, 226801 (2005).

- ¹⁴M. Büttiker, *IBM J. Res. Dev.* **32** 317 (1988).
- ¹⁵B. A. Bernevig, T. L. Hughes and S. C. Zhang, *Science* **314**, 1757 (2006).
- ¹⁶M. König, S. Wiedmann, C. Brüne, A. Roth, H. Buhmann, L. W. Molenkamp, X.-L. Qi, and S.-C. Zhang, *Science* **318**, 766 (2007).
- ¹⁷A. Roth, C. Brüne, H. Buhmann, L. W. Molenkamp, J. Maxiejko, X.-L. Qi, and S.-C. Zhang, *Science* **325**, 294 (2009).
- ¹⁸Currently, measurements of the QSH effect have only been conducted in the temperature range between 10 mK and 4 K. The actual temperature limits for HgTe QW structures have yet to be experimentally explored.
- ¹⁹B. Zhou, H.-Z. Lu, R.-L. Chu, S.-Q. Shen, and Q. Niu, *Phys. Rev. Lett.* **101**, 246807 (2008).
- ²⁰M. König, H. Buhmann, L. W. Molenkamp, T. Hughes, C.-X. Liu, X.-L. Qi, and S.-C. Zhang, *J. Phys. Soc. Jpn.* **77**, 031007 (2008).
- ²¹Y. S. Gui, C. R. Becker, N. Dai, J. Liu, Z. J. Qiu, E. G. Novik, M. Schäfer, X. Z. Shu, J. H. Chu, H. Buhmann, and L. W. Molenkamp, *Phys. Rev.* **70**, 115328 (2004).
- ²²J. Sinova, D. Culcer, Q. Niu, N. A. Sinitsyn, T. Jungwirth, and A. H. MacDonald, *Phys. Rev. Lett.* **92**, 126603 (2004).
- ²³Results are in preparation for publication.